MOLEKUL
eISSN: 2503-0310

Articles

https://doi.org/10.20884/1.jm.2024.19.3.11162

Preliminary Studi of Dye-Sensitized Solar Cell Photoelectrochemical for CO_2 Conversion to Methanol Using CuO-modified Dark TiO_2 Nanotubes Array as Cathode

Hany Dwi Arda, Muhammad Iqbal Syauqi*, Jarnuzi Gunlazuardi

Chemistry Department, Faculty of Mathematics and Natural Science, University of Indonesia, Depok, Indonesia

*Corresponding author email: muhammad.iqbal@sci.ui.ac.id

Received January 15, 2024; **Accepted** June 19, 2024; **Available online** November 20, 2024

ABSTRACT. The increased atmospheric carbon dioxide (CO_2) levels can lead to climate change and adversely affect human health. Therefore, it is necessary to develop a method to capture CO_2 and convert it into a more valuable substance, such as methanol. In this study, we established a tandem system involving dye-sensitized solar cells and photoelectrochemical (DSSC-PEC), which included the PEC zone using CuO/dark TiO_2 nanotube array (CuO/dTNA) as the dark cathode where CO_2 reduction takes place, and Co-Pi/blue TiO_2 nanotube array (Co-Pi/bTNA) as the counter photoanode. For the DSSC zone, N719/TNA was used as the photoanode, I^-/I_3^- electrolyte, and Pt/FTO as the cathode. The tandem system was constructed by connecting the PEC cathode to the DSSC photoanode and the PEC photoanode to the DSSC cathode using silver wire. Under solely visible light induction and water containing sodium bicarbonate electrolyte saturated with CO_2, the proposed devise produced methanol at 1.292 µmol/hour.

Keyword: Carbon dioxide, copper oxide, dark TiO_2 nanotube, DSSC-PEC

INTRODUCTION

The global average surface concentration of CO_2 increased by 2.13 ppm to reach 417.06 ppm, a rate similar to the one observed during the past decade. Atmospheric CO_2 is now 50% higher than pre-industrial levels (Kim et al., 2016). Increased atmospheric carbon dioxide (CO_2) levels can affect environmental health. Long-term exposure to high levels of CO_2 can affect cognitive performance, bone demineralization, stress, and endothelial dysfunction (Jacobson et al., 2019). One way to reduce CO_2 concentrations is to convert it into multi-carbon oxygenates and valuable products such as methane (CH_4), methanol (CH_3OH), etc (de Almeida et al., 2020; He & Janáky, 2020) using electrochemical CO_2 reduction reaction (CO_2RR) (Liu et al., 2022), and some other methods, such as photoelectrocatalysis.

TiO_2 is extensively employed as a semiconductor material, serving as an electrocatalyst and a photoelectrocatalyst for CO_2 reduction. This usage is attributed to its nontoxicity, affordability, and high chemical stability (Yuan et al., 2018). In addition, dark TiO_2 nanotube array (dTNA) shows improved optical absorption properties compared to white TiO_2 by the formation of oxygen vacancies, Ti^{3+} ions, structural disorder/defects on the surface, Ti-OH groups, and Ti-H groups (Andronic & Enesca, 2020). Due to the introduction of oxygen vacancies, the dark TiO_2-supported catalyst exhibited a considerably enhanced ability to adsorb CO_2, ultimately improving O_2 conversion (Jin et al., 2022).

Copper, identified as a heterogeneous catalyst, has demonstrated the capability to generate valuable hydrocarbons and alcohols through an electrochemical reduction reaction of CO_2 (Nitopi et al., 2019). Cu_2O with various morphologies can be an efficient electrocatalyst for CO_2 reduction to methanol in an aqueous medium, but it requires a high overpotential, -1.7 V vs NHE (Chang et al., 2009). Previous research discovered that a copper oxide and TiO_2 (CuO/TiO_2) catalyst could reduce CO_2 into multi-carbon oxygenates like ethanol, acetone, and n-propanol. This reaction had a maximum overall faradaic efficiency of 47.4% at a potential of -0.85 V vs. NHE, which improved CO_2 catalytic activity (Yuan et al., 2018).

Photoelectrochemical (PEC) is considered the most effective way to convert CO_2 into selective gases such as methane, ethane, etc., and liquid products such as methanol, ethanol, etc., under solar light irradiation, especially for liquid products (Kumaravel et al., 2020). In previous studies, tandem solar cells and photoelectrochemical systems have the advantage of high efficiency in converting photons to chemical compounds formed (Qin et al., 2013). Qin et al. (2013) designed a tandem system comprising dye-sensitized solar cells (DSSC) and TiO_2 photoelectrochemical cells (PEC) known as DSSC-PEC.

In this configuration, the PEC cell functioned as a catalyst zone for CO_2 conversion, while the DSSC cells utilized N719 dyes as photon absorbers, which is among the best photosensitizers used in TiO_2-based dye-sensitized solar cells (Qin et al., 2013).

The copper-doped titania catalysts for photocatalytic reduction of CO_2 (Slamet et al., 2005) and CuO-modified TiO_2 nanotube photoelectrode for water splitting have been reported (de Brito et al., 2018). In addition, converting CO_2 gas into methanol using cobalt phosphate/blue-TiO_2 nanotube arrays (CoPi/bTNA) electrodes as photoanode at photoelectrochemical was also reported (Ramadhani et al., 2023).

We report herein the construction of DSSC-PEC to convert CO_2 to methanol. The TNA/N719 was employed as a photoanode in the DSSC, where the PEC part employed a copper oxide-modified dark TiO_2 nanotube arrays (CuO/dTNA) as the dark anode coupled with CoPi/bTNA as the photoanode.

EXPERIMENTAL SECTION

Materials

Titanium metal plate, ethylene glycol, ammonium fluoride, acetone, ethanol, sodium hydroxide, sodium hydrogen carbonate, potassium phosphate, acetonitrile, N719 dyes, FTO (Flour Tin Oxide), potassium iodide, I_2, Nafion 117 membrane, copper nitrate, cobalt nitrate, and distilled water were purchased commercially. All materials were obtained from Sigma-Aldrich, except for the titanium plate (99.6% purity) obtained from Baoji Jinsheng Metal Material Co. Ltd.

Method

Amorphous titanium nanotube arrays (TNA) were prepared by anodizing titanium foil in an electrolyte solution containing 2.5 wt% H_2O and 0.2 wt% NH_4F in ethylene glycol for 1 hour under a constant potential of 50V at room temperature. The resulting amorphous TNA was then annealed at 450°C under atmospheric conditions at a rate of 5°C per minute for 2 hours to obtain the crystal phase of the TiO_2 Nanotube Array (TNA).

Amorphous dTNA (dark TNA) was fabricated by electrochemical reduction of amorphous TNA in 0.1 M NaOH electrolyte using a 3-electrode configuration comprising an amorphous TNA as the working electrode, a Pt wire as a counter electrode, and Ag/AgCl as a reference electrode for 5 min. Meanwhile, bTNA (blue TNA) was synthesized by electrochemically reducing TNA with 0.1M NaOH electrolytes for 20 minutes (Kim et al., 2016). The resulting amorphous dTNA was dipped into copper nitrate solution in water containing ethanol for 1 minute, pulled up, and dried at room temperature for 2 minutes to obtain CuO/dTNA. The dip-coating was repeated three times (Yang et al., 2018). The CuO/dTNA was heated at 450 °C under nitrogen at a 5°C/minute rate for 2 hours.

CoPi/bTNA was fabricated by electrodeposition method, where the bTNA was immersed in 0.5 mM cobalt nitrate containing 0.1M potassium phosphate) at pH 7 using a 3-electrode configuration comprising a bTNA as a working electrode, a Pt wire as a counter electrode, and Ag/AgCl as a reference electrode for 15 min (Stein, 2023).

The prepared materials were characterized using Shimadzu IR Prestige 2 for FTIR, X'pert PRO merk PANalitycal MPD PAW3040/60 for XRD, Zein EVO MO10 for SEM, electrochemical work station E-chem/EDaq for Linear Sweep Voltammetry (LSV) and Multi Pulse Amperometry (MPA).

The DSSC consists of N719-sensitized TiO_2 nanotubes (N719/TNA) as a photoanode, I^-/I_3^- as an electrolyte solution, and Pt/FTO as a counter electrode, which is arranged as a sandwich cell. To prepare the DSSC, the TNA was immersed in 300 µM N719 dye solution (ethanol as the solvent) for 24 hours. Subsequently, the N719-sensitized TNA was rinsed with ethanol and was left to dry in the air. The electrolyte solution of I^-/I_3^- was prepared by dissolving 0.13 g of I_2 crystals in a solvent mixture of 5 mL ethylene glycol and 20 mL acetonitrile. Following this, the 0.18 g of KI was added and the solution was stirred for 30 minutes. Pt/FTO was created by coating FTO glass with a drop of 20 mM H_2PtCl_6 solution in ethanol, dried in the air, and then heated at 380^0C for 30 minutes (Amelia & Gunlazuardi, 2023; Qin et al., 2013). For the construction of DSSC, N719/TNA and Pt/FTO are separated by parafilm spacers to form a sandwich cell, which is then filled with I^-/I_3^- electrolyte in acetylacetone (An'Nur et al., 2020).

In the PEC zone, CuO/dTNA material was employed as the dark cathode and CoPi/bTNA as the photoanode. Both electrodes were dipped into a glass reactor containing 100mL of $NaHCO_3$ electrolyte solution-saturated CO_2 pH 7 in the cathode zone and 0.1 M NaOH in the anode zone. The DSSC anode zone (N719/TNA) was connected to the PEC cathode, while the DSSC cathode zone (Pt/FTO) was connected to the potentiostat working electrode. The PEC anode zone was connected to the counter and reference electrode. During the CO_2 conversion, the DSSC and The photoanode in PEC were irradiated with a white LED lamp for 6 hours at room temperature. After the predetermined irradiation time, a sample of 10 mL was taken from the reactor every 2 hours to analyze the compounds formed from the reaction by the gas chromatic method (Ramadhani et al., 2023).

RESULTS AND DISCUSSIONS

This report will focus on preparing and characterizing the dark titanium oxide nanotube array composited by copper oxide (CuO/dTNA) and preliminary application in the DSSC-PEC device for CO_2 conversion. The CuO/dTNA was operated as the dark cathode in the PEC zone, where CO_2 conversion to methanol occurred.

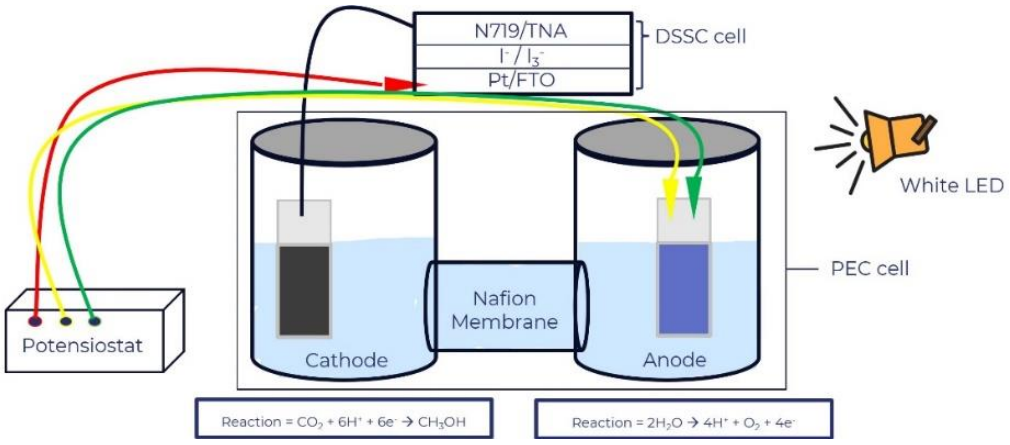

Figure 1. The schematic arrangement of the DSSC-PEC tandem for a photoelectrochemical CO_2 reduction

Characterization of Prepared CuO/dTNA Material

As shown in **Figure 2a**, all FTIR spectra show absorption peaks around 838 cm^{-1}, indicating the existence of the ~Ti-O-Ti~ network, which is typical for the occurrence of the crystalline phase of titanium dioxide. Slightly different peaks for dTNA were observed in that region due to the increasing population of Ti^{3+} (hence more defective oxygen). On the other hand, a more broadening peak was significantly observed in the CuO/dTNA, due to overlapping with the absorption peak of 603 cm^{-1}, indicating the presence of ~Cu-O-Cu~ network (Dong et al., 2017). The O-H bending (1662 cm^{-1}) and O-H stretching (3257 cm^{-1}) were observed in almost all spectra, though their intensity was different due to their population. A typical absorption peak in the 1380 – 1670 cm^{-1} range was observed in the CuO/TNA, which could be attributed to O-H bending vibrations in conjunction with copper atoms (Nair et al., 1991). The FTIR analysis suggests the formation of the CuO/dTNA composite, a conclusion that will be substantiated by the subsequent XRD characterization.

In addition, **Figure 2b** shows the diffractogram of TNA, dTNA, and CuO/dTNA. Based on ICDD data code 00-044-0706 (Kim et al., 2016; Pinto et al., 2019), all samples show characteristic diffraction patterns that indicate the presence of an anatase crystal phase. However, there are some differences at certain diffraction peaks. It was observed that there is a shift of typical anatase peaks towards larger 2θ, one of them is the peak in the range of 2θ 25.309° (for TNA) and 2θ 25.5247° (dTNA), due to increasing defect oxygen in the dTNA compared to TNA. Moreover, In the CuO/dTNA diffractogram, several additional peaks were observed at 2θ 23.0528, 35.3191, 53.2002, and 75.1793, indicating a typical CuO crystal phase. Unambiguously, this XRD characterization confirms the success of the CuO/dTNA preparation.

The morphological structure of CuO/dTNA was then further observed using SEM (**Figure 2c**). Based on the observation, it was noted that the nanotubes were arranged in an orderly and upright structure with an inner tube diameter of approximately 55.95 nm and a tube length of approximately 5.281 µm. On the surface of the nanotubes, it is observed that CuO nanoparticles are evenly distributed. The energy dispersive X-ray (EDX) analysis of CuO/dTNA shown in **Figure 2d** revealed the elemental composition of the sample of 23.7; 59; 4.2; and 13.1% for Ti, O, Cu, and C, respectively. Put into account the 1:2 ratio of Ti:O elements from the TiO_2 compound, as well as the 1:1 ratio of Cu:O compound (in accordance to the XRD data), the rest 7.4 atomic% of O might be attributed to the crystal defect from O-H surface of both CuO and TiO_2 terminals or might be in bond with the graphite in the form of graphite oxide (Pinto et al., 2019; Kim et al., 2016).

Electrochemical Behavior of CuO/dTNA

Cathodic Linear Sweep Voltammetry (LSV) was conducted using an electrochemical cell with the 3-electrode system in 0.1M $NaHCO_3$ with and without CO_2 saturation (at pH 7). The working electrode was composed of TNA, dTNA, and CuO/TNA, while a Pt wire served as the counter electrode, and Ag/AgCl as the reference electrode. The onset potentials (**Figure 3**) of TNA, dTNA, and CuO/dTNA in CO_2-saturated electrolytes were observed at -0.505, -0.184, and 0,026 V vs. Ag/AgCl, respectively. In comparison, the onset potential in electrolytes without CO_2 saturation was -0,555, -0.443, and -0,136 V Ag/AgCl, respectively. The more positive onset potential shows the favorability towards reduction reaction (Syauqi, 2023). As the CO_2 Reduction Reaction (CO_2RR) occurs in the water system, there will be competition with a more favourable hydrogen evolution reaction (HER) from water reduction. Thus, a more active catalyst towards CO_2RR is needed. The experiment with and without CO_2 saturation could estimate the catalyst activity to CO_2RR. As can be seen in **Figure 3**, there was a negligible change in onset potential and current density of TNA with and without CO_2 saturation. This result suggests that the pristine TNA was insufficient to be used as a catalyst for CO_2RR. On the other hand, dTNA shows a positive shift of onset potential along with an increase in the

current density after CO_2 saturation, showing the better activity of dTNA compared to TNA for CO_2RR. This might be caused by the increase of active oxygen vacancy on the surface of dTNA (Balog et al., 2021). Thus, the oxygen vacancy on the surface of dTNA and the unique effect of CuO are expected to elevate the activity of CO_2RR. It is interesting to explore more of this potential.

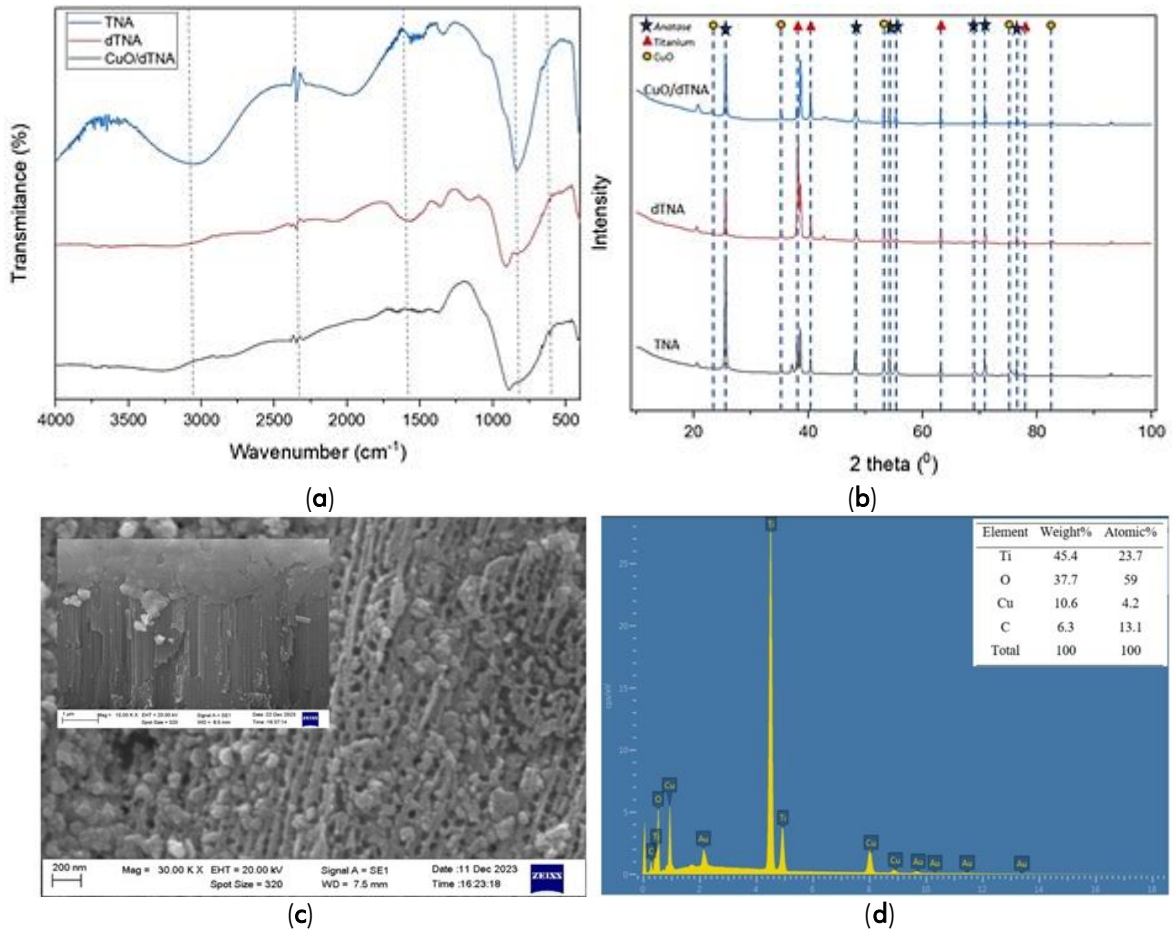

Figure 2. (a) FTIR characterization of TNA (blue); dTNA (red); and CuO/dTNA (black); (b) Diffractogram of TNA; dTNA; and CuO/dTNA; (c) SEM of CuO/dTNA. Inset is an enlargement of the cross-section view; (d) EDX spectra of CuO/dTNA

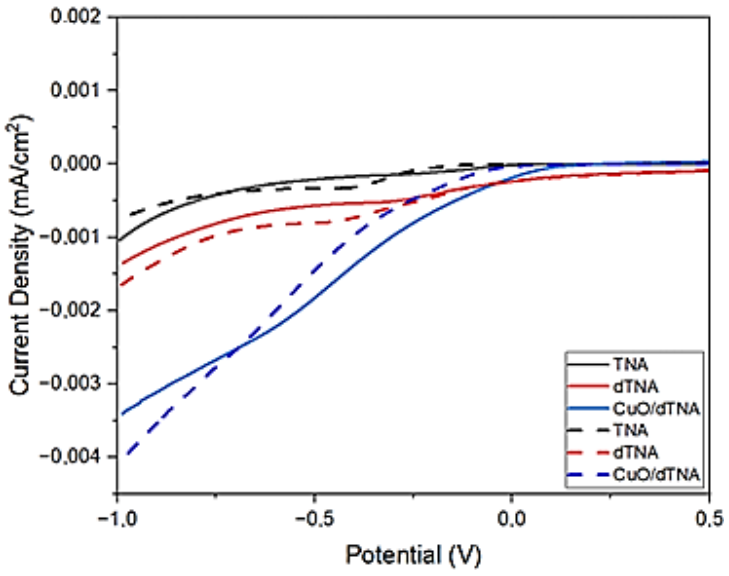

Figure 3. Cathodic Linear Sweep Voltammetry in electrolyte $NaHCO_3$ pH 7 saturated CO_2 (solid line) and no CO_2 (dash line) with a scan rate of 20 mV/s

Characterization of DSSC and Photoanode for DSSC-PEC Tandem System

The components of the DSSC were set up in a sandwich cell configuration with N719/TNA as the anode, Pt/FTO as the cathode, and electrolyte solution of I^-/I_3^-. A parafilm spacer was inserted between the cathode and anode to prevent any short circuits. The efficiency of DSSC was evaluated by plotting the current versus potential curve within the range of 0 to +1 V. **Figure 4** shows the current versus voltage curve of tested DSSC under visible light irradiation from a white LED lamp. From this curve, the parameters used to determine the efficiency of DSSC are the current produced (Jsc), the maximum current produced (Jmax), the voltage produced (Voc), the maximum voltage produced (Vmax), and the maximum power produced (Pmax) (Sharma et al., 2018). From this data, the Filling Factor (FF) and % DSSC efficiency (η) can be calculated using the following equation:

$$FF = \frac{V_{max} \times J_{max}}{V_{oc} \times J_{sc}}$$

$$\eta = \frac{FF \times J_{sc} \times V_{oc}}{P_{in}} \times 100\%$$

By using a lamp power of 29.1 W/m^2 for irradiation (P_{in}), and FF value of 0.46, the DSSC cell efficiency is 1.39%.

The self-constructed DSSC mentioned above was then arranged in tandem with the PEC zone. The PEC zone was comprised of CuO/dTNA dark cathode and CoPi/bTNA photoanode (See **Figure 1**). The CuO/dTNA in the tandem system operated as a dark working cathode where CO_2 reduction to methanol took place, while CoPi/bTNA served as a photoanode, facilitating the oxidation of water into electrons (e^-), oxygen, and protons (H^+) under visible light radiation occurred. The choice of the materials was based on the previous work reporting the effectivity of CoPi as a water oxidation catalyst (Esswein et al., 2011) and the match-up band energy of the N719/TNA tandem cell with the proposed photoelectrochemical cell (Neetu et al., 2017).

The CoPi/bTNA was characterized as photoanode using the LSV method to analyze the current density when given a potential difference that changes linearly within a certain range under conditions of visible light with a white LED lamp in an electrochemical cell with a 3-electrode system. **Figure 5a** shows the curve of LSV TNA and CoPi/bTNA. The curve shows that the Oxygen Evolution Reaction (OER) potential of CoPi/bTNA is 0.76V, clearly showing superior OER activity compared to the bare TNA. In addition, the multipulse amperometry (MPA) experiment at 0 V vs Ag/AgCl with chopped light was conducted and shown in **Figure 5b**. It can be seen that CoPi/bTNA gives a 7-fold increase in photocurrent compared to bare TNA when exposed to visible light. The higher current density response was due to the contribution of reduction TNA into bTNA-formed Ti^{3+} on the surface TiO_2 nanotubes (Peighambardoust & Aydemir, 2020) and the CoPi catalyst enhancing the surface properties of hole-electron transfer (Ma et al., 2015).

Tandem System for CO_2 Reduction

The schematic of the tandem DSSC-PEC system can be seen in **Figure 1**. The process of converting CO_2 into methanol was conducted using a H-type reactor employing the DSSC-PEC system. The CO_2 conversion to methanol production is presented in terms of the amount of methanol produced for 6 hours. Where 10 mL of sample was taken every 2 hours. In the PEC anode, electrons on the CoPi/bTNA photoanode will be excited to the conduction band and then transferred to the Pt/FTO as the DSSC cathode through the external circuit. The electrons that go to the cathode will leave holes (h^+) on the anode surface, which will oxidize water into oxygen while producing electrons (e^-) and protons (H^+) that will be used for the cathodic reaction. H^+ ions produced at the anode will travel through the nafion membrane to the PEC cathode, while the electron will travel to DSSC to regenerate the excited dye. The electron generated by the DSSC will be transferred to the CuO/dTNA cathode, where the CO_2 reduction reaction to methanol occurs.

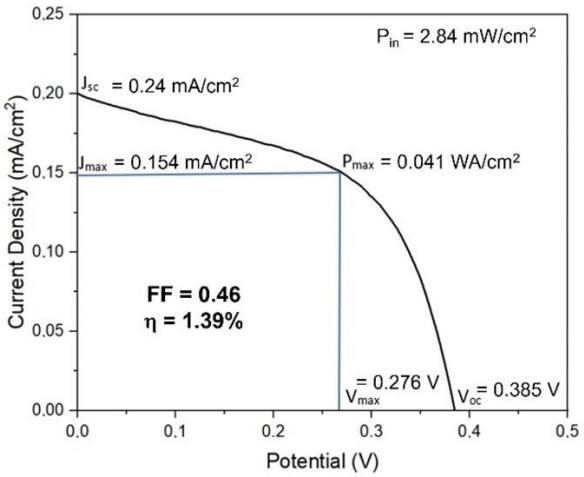

Figure 4. The plot of current versus voltage of the DSSC zone.

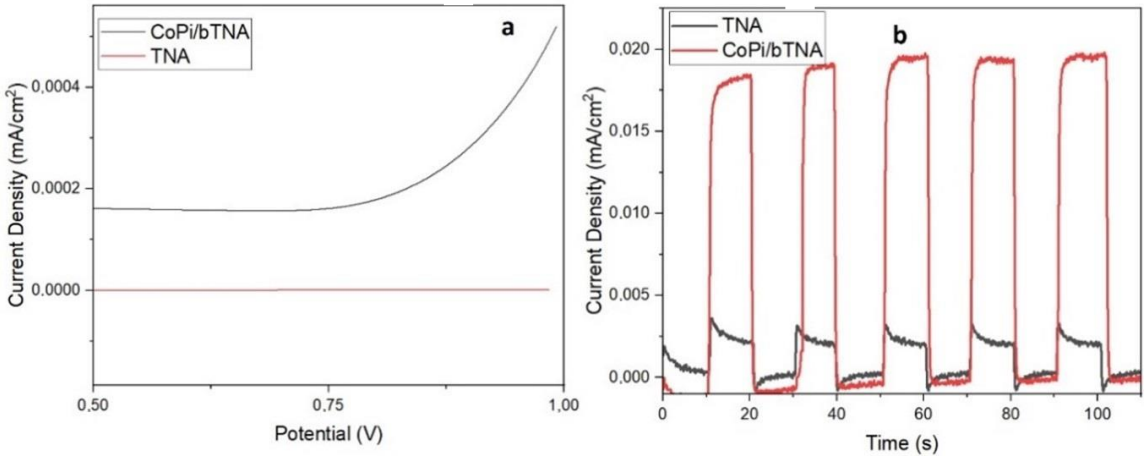

a b

Figure 5. (**a**) LSV of CoPi/bTNA and TNA with scan rate 20 mV/s; and (**b**) MPA of CoPi/bTNA and TNA at 0 V vs Ag/AgCl, all recorded under white LED lamp illumination in 0.1 M NaOH solution.

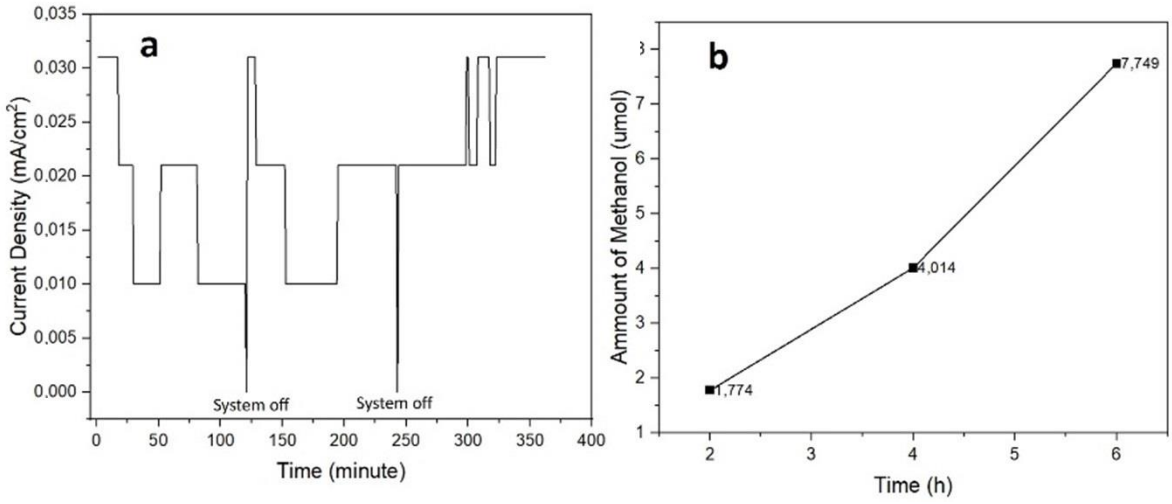

a b

Figure 6. (**a**) The current versus time curve of CO_2 reduction in tandem system; and (**b**) Amount of methanol produced in DSSC-PEC tandem system.

Figure 6a shows experimental data on current density during the system. From this data, the average current density for 2 hours, 4 hours, and 6 hours are 0.0186, 0.0208, and 0.026 mA/cm^2, respectively. According to Faradaic law, if this current is used entirely to convert CO_2 into methanol, the theoretical amount of methanol obtained will be 8.327, 18.623, and 34.918 µmol. However, the experimental results shown in **Figure 6b** give a different amount of methanol generated from the theoretical value. The methanol produced increased with increasing reaction time with 1.774, 4.014, and 7.749 µmol for 2, 4, and 6 hours, respectively. It is possible that other products, such as ethanol, propanol, and more by-products, are formed along with methanol.

CONCLUSIONS

In conclusion, the modification of the TiO_2 nanotube array by two steps of electroreduction and copper oxide incorporation was successfully performed. Characterization of the electrode by FTIR, XRD, and SEM revealed the formation of CuO on the surface of the dark TiO_2 nanotube array. The FTIR analysis exhibited an absorption peak FTIR of 603 cm^{-1}, indicative of the ~Cu-O-Cu~ network formation. Additionally, the diffractogram of the CuO/dTNA displayed several additional peaks observed at 2θ 23.0528, 35.3191, 53.2002, and 75.1793, indicating a typical CuO crystal phase. SEM imaging further demonstrated the uniform distribution of CuO nanoparticles on the surface of dTNA. Furthermore, cathodic linear sweep voltammetry highlighted the potential of the CuO/dTNA electrode as an electrocatalyst for CO_2 reduction reaction based on the improved onset potential and increased current density. In addition, when applied as a dark cathode along with CoPi/bTNA photoanode in the PEC system coupled with a DSSC to conduct a CO_2 reduction reaction, the system was able to produce methanol with 1.292 µmol/hour production rate.

REFERENCES

Amelia, P., & Gunlazuardi, J. (2023). Development of $BiOBr/TiO_2$ nanotube electrode for conversion of nitrogen to ammonia in a tandem photoelectrochemical cell under visible light. *International Journal of Renewable Energy Development*, *12*(4), 702–710. https://doi.org/10.14710/ijred.2023.51314

Andronic, L., & Enesca, A. (2020). Black TiO_2 Synthesis by Chemical Reduction Methods for Photocatalysis Applications. *Frontiers in Chemistry*, *8,* 565489. https://doi.org/10.3389/fchem.2020.565489

An'Nur, F. K., Wihelmina, B. V., Gunlazuardi, J., & Wibowo, R. (2020). Tandem system of dyes sensitized solar cell-photo electrochemical (DSSC-PEC) employing TiO_2 nanotube/BiOBr as dark cathode for nitrogen fixation. *AIP Conference Proceedings*, *2243*, 020002. https://doi.org/10.1063/5.0001100

Balog, Á., Samu, G. F., Petö, S., & Janáky, C. (2021). The mystery of black TiO_2: Insights from combined surface science and in situ electrochemical methods. *ACS Materials Au*, *1*(2), 157–168. https://doi.org/10.1021/acsmaterialsau.1c00020

Chang, T.-Y., Liang, R.-M., Wu, P.-W., Chen, J.-Y., & Hsieh, Y.-C. (2009). Electrochemical reduction of CO_2 by Cu_2O-catalyzed carbon clothes. *Materials Letters*, *63*(12), 1001–1003. https://doi.org/10.1016/j.matlet.2009.01.067

de Almeida, J., Pacheco, M. S., de Brito, J. F., & de Arruda Rodrigues, C. (2020). Contribution of Cu_xO distribution, shape, and ratio on TiO_2 nanotubes to improve methanol production from CO_2 photoelectroreduction. *Journal of Solid State Electrochemistry*, *24*, 3013–3028. https://doi.org/10.1007/s10008-020-04739-3

de Brito, J. F., Tavella, F., Genovese, C., Ampelli, C., Zanoni, M. V. B., Centi, G., & Perathoner, S. (2018). Role of CuO in the modification of the photocatalytic water splitting behavior of TiO_2 nanotube thin films. *Applied Catalysis B: Environmental*, *224*, 136–145. https://doi.org/10.1016/j.apcatb.2017.09.071

Dong, C.-D., Chen, C.-W., Kao, C.-M., & Hung, C.-M. (2017). Synthesis, characterization, and application of CuO-modified TiO_2 electrode exemplified for ammonia electro-oxidation. *Process Safety and Environmental Protection*, *112*, 243–253. https://doi.org/10.1016/j.psep.2017.05.016

He, J., & Janáky, C. (2020). Recent advances in solar-driven carbon dioxide conversion: Expectations versus reality. *ACS Energy Letters*, *5*(6), 1996–2014. https://dx.doi.org/10.1021/acsenergylett.0c00645?ref=pdf

Jacobson, T. A., Kler, J. S., Hernke, M. T., Braun, R. K., Meyer, K. C., & Funk, W. E. (2019). Direct human health risks of increased atmospheric carbon dioxide. *Nature Sustainability 2,* 691–701. https://doi.org/10.1038/s41893-019-0323-1

Jin, B., Ye, X., Zhong, H., Jin, F., & Hu, Y. H. (2022). Enhanced photocatalytic CO_2 hydrogenation with wide-spectrum utilization over black TiO_2-supported catalyst. *Chinese Chemical Letters*, *33*(2), 812–816. https://doi.org/10.1016/j.cclet.2021.07.046

Kim, C., Kim, S., Hong, S. P., Lee, J., & Yoon, J. (2016). Effect of doping level of colored TiO_2 nanotube arrays fabricated by electrochemical self-doping on electrochemical properties. *Physical Chemistry Chemical Physics*, *18*(21), 14370–14375. https://doi.org/10.1039/c6cp01799a

Kumaravel, V., Bartlett, J., & Pillai, S. C. (2020). Photoelectrochemical conversion of carbon dioxide (CO_2) into fuels and value-added products. *ACS Energy Letters*, 5(2), 486–519. https://doi.org/10.1021/acsenergylett.9b02585

Liu, W., Zhai, P., Li, A., Wei, B., Si, K., Wei, Y., Wang, X., Zhu, G., Chen, Q., Gu, X., Zhang, R., Zhou, W., & Gong, Y. (2022). Electrochemical CO_2 reduction to ethylene by ultrathin CuO nanoplate arrays. *Nature Communications*, *13*(1), 1877. https://doi.org/10.1038/s41467-022-29428-9

Ma, Y., Le Formal, F., Kafizas, A., Pendlebury, S. R., & Durrant, J. R. (2015). Efficient suppression of back electron/hole recombination in cobalt phosphate surface-modified undoped bismuth vanadate photoanodes. *Journal of Materials Chemistry A*, *3*(41), 20649–20657. https://doi.org/10.1039/C5TA05826K

Nair, C. G. R., Mathew, S., & Ninan, K. N. (1991). Thermoanalytical investigations on kinetics and mechanism of deamination of tris(ethylenediamine)copper(II) sulphate. *Journal of Thermal Analysis*, *37*(10), 2325–2334. https://doi.org/10.1007/BF01913732/METRICS

Neetu, Maurya, I. C., Singh, S., Gupta, A. K., Srivastava, P., & Bahadur, L. (2017). N/Al-incorporated TiO_2 nanocomposites for improved device performance of a dye-sensitized solar cell. *ChemistrySelect*, *2*(15), 4267–4276. https://doi.org/10.1002/SLCT.201700550

Nitopi, S., Bertheussen, E., Scott, S. B., Liu, X., Engstfeld, A. K., Horch, S., Seger, B., Stephens, I. E. L., Chan, K., Hahn, C., Nørskov, J. K., Jaramillo, T. F., & Chorkendorff, I. (2019). Progress and perspectives of electrochemical CO_2 reduction on copper in aqueous electrolyte. *Chemical Reviews*, *119*(12), 7610–7672. https://doi.org/10.1021/acs.chemrev.8b00705

Peighambardoust, N. S., & Aydemir, U. (2020). Blue TiO_2 nanotube arrays as semimetallic materials with enhanced photoelectrochemical activity towards water splitting. *Turkish Journal of Chemistry*, *44*(6), 1642. https://doi.org/10.3906/KIM-2004-85

Pinto, F. M., Suzuki, V. Y., Silva, R. C., & La Porta, F. A. (2019). Oxygen defects and surface chemistry of reducible oxides. *Frontiers in Materials*, *6*, 466671. https://doi.org/10.3389/FMATS.2019.00260/BIBTEX

Qin, G., Zhang, Y., Ke, X., Tong, X., Sun, Z., Liang, M., & Xue, S. (2013). Photocatalytic reduction of carbon dioxide to formic acid, formaldehyde, and methanol using dye-sensitized TiO_2 film. *Applied Catalysis B: Environmental*, *129*, 599–605. https://doi.org/10.1016/j.apcatb.2012.10.012

Ramadhani, F. F., Gunlazuardi, J., Wibowo, R., & Abdullah, I. (2023). *Photoelectrochemical CO_2 conversion to CH_3OH with photoanode Blue-TNA/CoPi*. https://lib.ui.ac.id/m/detail.jsp?id=9999920519334&lokasi=lokal

Sharma, K., Sharma, V., & Sharma, S. S. (2018). Dye-sensitized solar cells: Fundamentals and current status. *Nanoscale Research Letters*, *13*(1), 381. https://doi.org/10.1186/s11671-018-2760-6

Stein, T. (2023). Greenhouse gases continued to increase rapidly in 2022. *National Oceanic and Atmospheric Administration U.S. Department of Commerce*. https://www.noaa.gov/news-release/greenhouse-gases-continued-to-increase-rapidly-in-2022

Syauqi, M. I., Cahyani, A. T., Putri, Y. M. T. A., & Jiwanti, P. K. (2023). Electroreduction of carbon dioxide (CO_2) with flow cell system using tin-modified copper foam electrode. *Environmental and Materials*, *1*(2). https://doi.org/10.61511/eam.v1i2.2023.363

Yang, Y., Kao, L. C., Liu, Y., Sun, K., Yu, H., Guo, J., Liou, S. Y. H., & Hoffmann, M. R. (2018). Cobalt-doped black TiO_2 nanotube array as a stable anode for oxygen evolution and electrochemical wastewater treatment. *ACS Catalysis*, *8*(5), 4278–4287. https://doi.org/10.1021/acscatal.7b04340

Yuan, J., Zhang, J.-J., Yang, M.-P., Meng, W.-J., Wang, H., & Lu, J.-X. (2018). CuO nanoparticles supported on tio_2 with high efficiency for CO_2 electrochemical reduction to ethanol. *Catalysts*, *8*(4), 171. https://doi.org/10.3390/catal8040171